Three-Dimensional Simulation of TiN Magnetron Sputter Deposition

Wolfgang Pyka
Institute for Microelectronics
TU Vienna
A-1040 Vienna, Austria
pyka@iue.tuwien.ac.at

Siegfried Selberherr
Institute for Microelectronics
TU Vienna
A-1040 Vienna, Austria
selberherr@iue.tuwien.ac.at

Abstract

We simulate the DC-magnetron sputter deposition of TiN-films to investigate the quality of the coverage and the uniformity of the film profiles. Reactor conditions are approximated by fitting an analytical function to angular distributions resulting from Monte Carlo calculations. Several positions on the wafer are simulated by setting the polar and azimuthal angle of the origin of the particle distribution function. Simulations are performed for a series of contact holes with diameters ranging from 0.3 μm to 1.0 μm and for a damascene structure. Simulation results are compared with experimental SEM pictures.

1. Introduction

In current integrated circuits technology thin barrier layers are used to improve and to optimize the properties of contacts, vias, and interconnect structures. The knowledge about film thicknesses which vary with process parameters and with the topography of the applied structures, and the achievement of good film conformality and step coverage are the most important tasks for choosing an appropriate deposition technique. Since Chemical Vapor Deposition (CVD) techniques [1] or approaches with collimated sputtering of titanium and titanium nitride films [2] could not yet supersede the well established Physical Vapor Deposition (PVD) processes such as magnetron sputtering, it is necessary to carefully investigate this deposition technique and extend it to the limit of its applicability.

We describe how simulation of titanium nitride (TiN) magnetron sputtering gives a deeper insight into the geometry and particle distribution conditions and the evolution of the layer profile. TiN is chosen because among other materials, it has been recognized as excellent barrier material and is used as nucleation/glue layer at the contact/via level as well as a diffusion barrier and anti-reflection coating in the interconnect stack [3].

2. Simulation

For the simulation we use a cell-based structuring element algorithm derived from image processing [4]. The geometry is represented by a cellular structure and a material index is assigned to each cell. The deposition rate $\vec{v}_d$ for each surface cell is obtained by the integration of a given particle

distribution function $F(\vartheta)$ over the solid angle Ω visible for the actual position

$$\vec{v}_d = \frac{R}{N} \int_{\Omega} F(\vartheta)\, \mathrm{d}\Omega\,, \qquad (1)$$

with the macroscopic deposition rate R and the normalizing factor N,

$$N = \int_{2\pi} F(\vartheta)\, \mathrm{d}\Omega\,, \qquad (2)$$

which ensures that for a flat, unshadowed surface the integrated deposition rate equals the macroscopic deposition rate R. The length of $\vec{v}_d$ corresponds to the deposition velocity whereas the direction of the deposition vector $\vec{v}_d$ represents the growth direction for the considered surface cell.

3. Particle Distribution Model

The resulting profile strongly depends on the visibility conditions of the simulated geometry and the distribution function. Both, the flux of the particles arriving at the wafer surface as well as the position on the wafer affect the behavior of the incident particles. We approximate the sputter conditions by fitting an exponential function

$$F(\vartheta) = a\vartheta^3 e^{-b\vartheta} \qquad (3)$$

to the angular distributions resulting from Monte Carlo simulations of sputtering particle transport [5]. The position of the maximum and the width of the peak of the exponential function are fitted to the flow conditions in the reaction chamber. For the three-dimensional simulation we assume that the function is radially symmetric. Additionally it is possible to add a variable isotropic fraction to take into account that the flow conditions slightly differ between the top surface and the bottom of the contact holes.

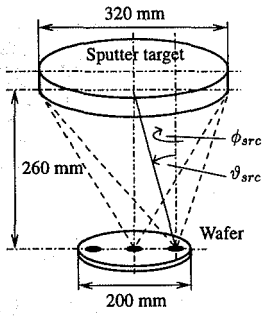

Figure 1. Experimental arrangement and location of the simulated structures.

4. Reactor Geometry

We simulate the deposition at several wafer positions by tilting the flux function by a polar angle ϕ_{src} and an azimuthal angle ϑ_{src} as depicted in Figure 1.

The polar angle ϕ_{src} and the azimuthal angle ϑ_{src} determine the origin of the particle distribution function. For the radially symmetric circular contact holes the simulation results are independent of ϕ_{src} but vary with ϑ_{src}. For the damascene structure the polar angle ϕ_{src} has to be considered, because the characteristic of the flux depends on the orientation of the main particle incidence with respect to the trench.

5. Input Geometries

We have performed simulations for different geometries. The geometries are composed with a solid modeling program based on the same cellular data representation as used for the topography simulation.

The input geometry for the contact hole structure are extracted from SEM pictures and imitated with the solid modeling program. The structure consists of circular holes with slanted sidewalls in a silicon-dioxide on silicon structure. A series of diameters ranging from 0.3 μm up to 1.0 μm

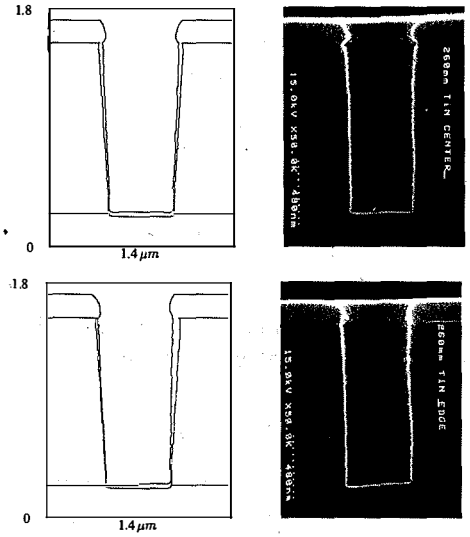

Figure 2. Deposition of TiN into a 0.5 μm diameter and 1.3 μm deep contact hole structure.

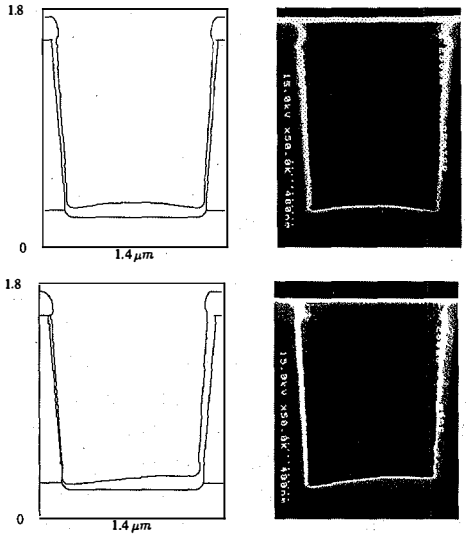

Figure 3. Deposition of TiN into a 1.0 μm diameter contact hole.

is simulated. For the larger diameters the structures are rounded at the bottom. The input geometries can be seen in the cross-sections of the simulation results in Figures 2 and 3.

The damascene structure consists of a 0.3 μm diameter, 0.7 μm deep hole in a 0.3 μm wide, 0.5 μm deep rectangular trench and is also built with the solid modeling program.

6. Results

6.1. Contact Holes

Figures 2 and 3 show the results of TiN-deposition into 0.5 μm and 1.0 μm diameter contact holes. The deposition rate is 33.8 nm/min and the simulation time is 320 s. The figures on the top are for structures located 260 mm below the center of the sputter target disk. The resulting structure is axially symmetric and agrees well with the corresponding SEM picture. The deposition at a position 90 mm off the wafer center for the same geometries is performed by a 20° azimuthal offset of the distribution function and the result is depicted in the lower row of Figures 2 and 3. The asymmetric profile reflects the slanted angle of the principle particle incidence. Note the small bulge at the topmost edge of the contact hole visible in the SEM pictures, which is reproduced in the simulations.

6.2. Damascene Structures

Finally, Figure 4 illustrates the results of TiN-deposition into a damascene structure with a circular hole within a rectangular trench with the same flux parameters as in the simulations above. Both simulations are for off center positions with $\vartheta_{src} = 20°$. In the upper row the polar direction of the main particle incidence is perpendicular to the trench, whereas below it is parallel. Cross-sections parallel to the trench on the left as well as perpendicular to the trench on

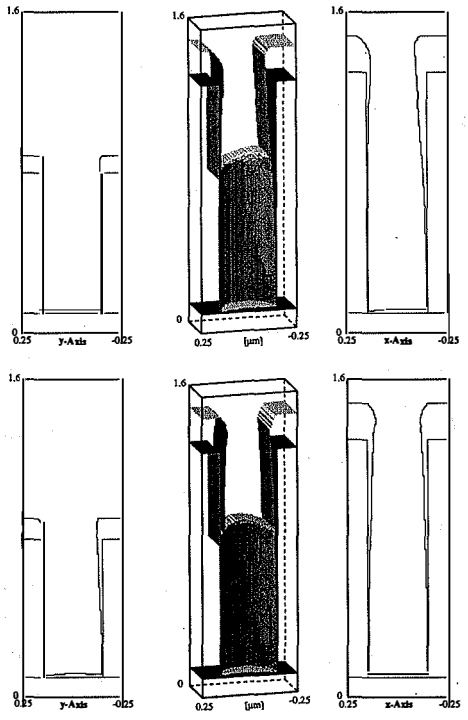

Figure 4. Damascene structure - perpendicular and parallel particle incidence.

the right are shown. The three-dimensional view and the corresponding cross-sections reflect the dependence on the polar direction and underline the necessity of a fully three-dimensional simulation of the deposition.

7. Conclusion

The analytical particle distribution model and the model of arbitrary location of the sputter target by setting its position by the angles ϕ_{src} and ϑ_{src} are capable of reproducing the film profiles including bulges obtained from experimental investigations. The selected analytical function is a good representation of the particle incidence conditions at the wafer surface. For all cases investigated, the bottom coverage is satisfying even for the $0.3\,\mu m$ diameter holes in the damascene structure. Due to the line of sight type sputter deposition care has to be taken for the sidewall coverage. Especially for the off-center positions the layer thickness at the shadowed sidewalls may be insufficient and the uniformity for all locations on the wafer is not guaranteed.

8. Acknowledgment

This research project is supported by SONY Corporation Atsugi Technology Center, Atsugi. Japan, Austria Mikro Systeme International AG, Unterpremstätten, Austria and Christian Doppler Forschungsgesellschaft, Vienna, Austria.

[1] C. Faltermeier, C. Goldberg, M. Jones, A. Upham, D. Manger, G. Peterson, J. Lau, A. E. Kaloyeros, B. Arkles, and A. Paranjpe, "Barrier Properties of Titanium Nitride Films Grown by Low Temperature Chemical Vapor Deposition from Titanium Tetraiodide," *J.Electrochem.Soc.*, vol. 144, no. 3, pp. 1002–1008, 1997.

[2] J. G. Ryan, S. B. Brodsky, T. Katata, M. Honda, N. Shoda, and H. Aochi, "Collimated sputtering of Titanium and Titanium Nitride Films," *MRS Bulletin*, vol. 20, no. 11, pp. 42–45, 1995.

[3] M. Eizenberg, "Chemical Vapor Deposition of TiN for Sub-0.5 μm ULSI Circuits," *MRS Bulletin*, vol. 20, no. 11, pp. 38–41, 1995.

[4] E. Strasser and S. Selberherr, "Algorithms and Models for Cellular Based Topography Simulation," *IEEE Trans.Computer-Aided Design*, vol. 14, no. 9, pp. 1104–1114, 1995.

[5] A. Myers, J. Doyle, and J. Abelson, "Monte Carlo Simulations of Magnetron Sputtering Particle Transport," *J. Vac. Sci. Technol. A*, vol. 9, no. 3, pp. 614–618, 1991.